Available online at www.sciencedirect.com
ScienceDirect
Journal of Crystal Growth 310 (2008) 777–782
JOURNAL OF CRYSTAL GROWTH
www.elsevier.com/locate/jcrysgro

Growth of *a*-plane ZnO thin films on $LaAlO_3(1\,0\,0)$ substrate by metal-organic chemical vapor deposition

Jr-Sheng Tian[a], Mei-Hui Liang[b], Yen-Teng Ho[c], Yuan-An Liu[a], Li Chang[a,*]

[a]*Department of Materials Science and Engineering, National Chiao Tung University, Hsinchu, Taiwan*
[b]*Center of General Education, Chung-Hua University, Hsinchu, Taiwan*
[c]*Chung-Shan Institute of Science and Technology, Longtan, Taoyuan, Taiwan*

Received 15 October 2007; accepted 7 November 2007
Communicated by R. Kern
Available online 21 November 2007

Abstract

ZnO($1\,1\,\bar{2}\,0$) thin films were successfully grown on $LaAlO_3$ (lanthanum aluminate) ($1\,0\,0$) substrate by atmospheric pressure metal-organic chemical vapor deposition. X-ray diffraction, atomic force microscopy, and scanning electron microscopy showed that ZnO films formed at 450 °C were composed of almost all ($1\,1\,\bar{2}\,0$) oriented grains while ($0\,0\,0\,2$) oriented ZnO grains started to appear at temperature above 550 °C. The *a*-plane ZnO films consisted of two types of domains with their *c*-axis perpendicular to each other due to $LaAlO_3(1\,0\,0)$ symmetry with low lattice mismatch along $\langle 1\,1\,0 \rangle$.
© 2007 Elsevier B.V. All rights reserved.

PACS: 78.55.Et; 68.55.−a; 61.10.−I; 81.15.Gh

Keywords: A1. High resolution x-ray diffraction; A3. Metalorganic chemical vapor deposition; B1. Oxides; B2. Semiconducting II-VI materials

1. Introduction

ZnO of wurtzite structure with $P6_3mc$ space group and lattice parameters of $a = 3.249$ Å and $c = 5.204$ Å is an attractive material because of the multi-functional applications for transparent electrodes, surface acoustic wave devices, and photoelectric devices, etc. The main advantages of ZnO are a wide direct band gap (3.3 eV) and a large exciton binding energy (60 meV at room temperature). Due to the larger exciton binding energy than GaN (25 meV), ZnO has better lasing efficiency than GaN. In recent years, research on epitaxy of ZnO has made remarkable advance on growth of high-quality *c*-plane ZnO thin films on *a*-plane [1,2] and *c*-plane sapphire substrates [3,4]. As ZnO has no inversion symmetry, ZnO crystal along the *c*-axis has alternate zinc ion (Zn^{2+}) layers with oxygen ion (O^{2-}) layers, which cause polarization in [0 0 0 1] and limit its applications for optical devices of light emitting diodes and laser diodes. For better luminescence characteristics, non-polar ZnO is preferred. Recently, growth of non-polar ZnO has therefore attracted much attention. It has been shown that non-polar ZnO($1\,1\,\bar{2}\,0$) and ($1\,0\,\bar{1}\,0$) (or *a*-plane and *m*-plane) can be epitaxially grown on *r*-plane sapphire and *m*-plane sapphire substrates with various growth techniques, such as molecular beam epitaxy, pulsed laser deposition (PLD) [5], and metal-organic chemical vapor deposition (MOCVD) [6,7]. However, formation of ZnO($0\,0\,0\,2$) grains may occur at low growth temperatures. Interestingly, Bellingeri et al. [8] have reported that from 550 to 870 °C ZnO($1\,1\,\bar{2}\,0$) thin films can be deposited on perovskite-structured $SrTiO_3(1\,0\,0)$ by PLD due to similar planar lattice with small lattice mismatch. Wei et al. [9] also showed similar results. Karger and Schilling observed that Al-doped ZnO($1\,1\,\bar{2}\,0$) was grown on TiO_2-terminated $SrTiO_3(1\,0\,0)$ at growth temperature up to 750 °C and lost its texture above 800 °C after 15 monolayers growth by PLD [10].

$LaAlO_3$ (lanthanum aluminate, LAO) has also perovskite-like structure (pseudo-cubic, $a = 3.791$ Å at room

*Corresponding author. Tel.: +886 3 5731615; fax: +886 3 5724727.
E-mail address: lichang@cc.nctu.edu.tw (L. Chang).

0022-0248/$ - see front matter © 2007 Elsevier B.V. All rights reserved.
doi:10.1016/j.jcrysgro.2007.11.073

temperature) with space group $R\bar{3}c$ at room temperature. In the rhombohedral structure, lattice parameter of LAO is 3.791 Å and $\alpha = \beta = \gamma = 90.066^\circ$. LAO undergoes second-order transition into cubic structure with space group $Pm\bar{3}m$ at temperature reaching about 400–500 °C [11–14]. During the cooling transition from cubic to rhombohedral structure, a lot of {1 0 0} twins with a twin angle of 0.18° and {1 1 0} twins with a twin angle of 0.25° are formed to release strains [15]. LAO has a large dielectric constant, and it has often been used as the substrate for growth of epitaxial high-temperature superconductor thin films. Growth of ZnO on LAO has never been reported, while non-polar ZnO has been grown on $SrTiO_3$ of perovoskite structure [8–10]. In this study, we report that growth of ZnO on LAO(1 0 0) substrate results in strongly *a*-plane oriented ZnO thin films by MOCVD.

2. Experimental procedure

Before deposition, as-received LAO substrates were cut into a size of $0.7 \times 1\,cm^2$ and then ultrasonically cleaned in a mixed solution of acetone and methanol for 5 min. After cleaning and drying by nitrogen blow, the LAO substrate was placed into a vertical MOCVD reactor and heated slowly with nitrogen flow to sweep probably any residual contaminations away. After the substrate reached to the growth temperature, the nitrogen flow was switched off, followed by the introduction of oxygen into the chamber for 10 min to stabilize oxygen atmosphere before the deposition. Then ZnO thin films were grown at various temperatures from 450 to 600 °C. In the atmospheric pressure MOCVD, oxygen gas used as the oxygen source, and the precursor of zinc acetylacetonate ($Zn(acac)_2$, 99.995%) was heated at 124 °C before introduction into the chamber by the carrier gas of nitrogen, which was separated from oxygen flow before reaching the substrate surface. The flow of carrier gas and oxygen gas was 150 and 250 sccm, respectively.

Structural characterization of ZnO thin films was carried out using X-ray (Cu Kα radiation) diffraction (XRD) method. The structural quality of ZnO thin films and in-plane relationships between LAO substrate and ZnO thin films were investigated by high-resolution X-ray (Cu $K\alpha_1$) diffraction (HRXRD) in ω-scan (rocking curve) and φ-scan. Tapping-mode atomic force microscope and scanning electron microscope were used to examine the topography of ZnO thin films.

3. Results and discussion

In Fig. 1(a), the XRD pattern shows that ZnO thin films grown at 450 °C exhibit only (1 1 $\bar{2}$ 0) reflection. For 550 °C growth, a very small ZnO(0 0 0 2) peak appears, and the peak intensity of (0 0 0 2) reflection increases for deposition at 600 °C, as shown in Fig. 1(b) and (c). The XRD patterns illustrate that (1 1 $\bar{2}$ 0) reflection is the dominant peak in all the films grown at temperature from 450 to 600 °C, while

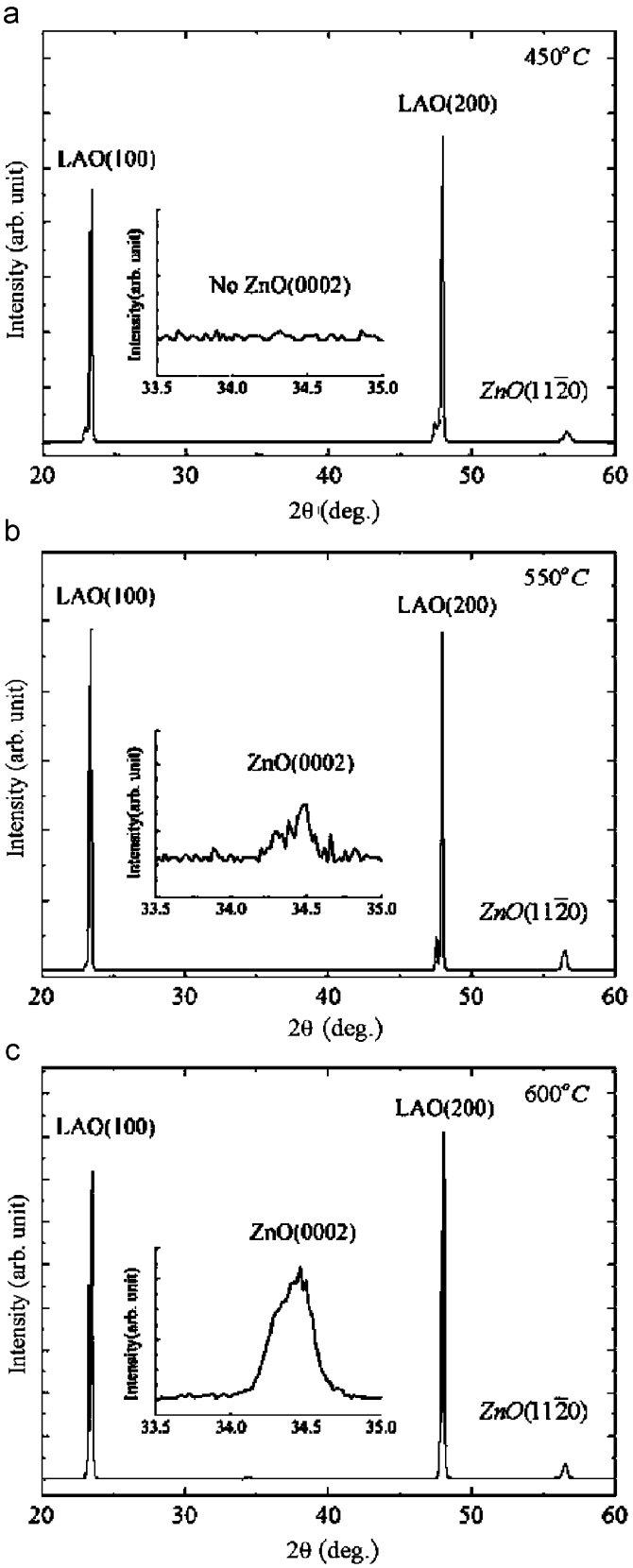

Fig. 1. θ–2θ XRD patterns of ZnO films deposited on LAO(1 0 0) substrates at growth temperature of (a) 450 °C, (b) 550 °C, and (c) 600 °C.

the intensity of (0 0 0 2) ZnO increases with the growth temperature. Similar results have been reported for (1 1 $\bar{2}$ 0) ZnO deposition on $SrTiO_3$(1 0 0) substrates [8–10].

The XRD φ-scan in Fig. 2(a) shows that there are four split peaks adjacently separated about 90°. The split angle in each peak is about 4°. Due to the square lattice of LAO(1 0 0), the four-fold symmetry may cause the ZnO being deposited in four in-plane orientations. The detailed analysis given on the following actually shows that there are two sets of ZnO{1 0 $\bar{1}$ 1} in the φ-scan. To determine those ZnO{1 0 $\bar{1}$ 1} peaks, the φ angle between them has to be known first. From geometric relationship, the φ angle is determined by projecting the plane normals of ZnO{1 0 $\bar{1}$ 1} on a surface parallel to ZnO(1 1 $\bar{2}$ 0). Because all ZnO {1 0 $\bar{1}$ 1} have the same angle with ZnO(1 1 $\bar{2}$ 0), the four projected points of normal directions of ZnO{1 0 $\bar{1}$ 1} are on a circle with the ZnO(1 1 $\bar{2}$ 0) projected point as the center of circle, as shown in Fig. 2(b). The angle between $(h_1 k_1 l_1)$ and $(h_2 k_2 l_2)$ of hexagonal lattice is given by Eq. (1), and the φ angle between any two of {1 0 $\bar{1}$ 1} projection directions on the (1 1 $\bar{2}$ 0) with its normal as zone axis can be solved from Eq. (2) where θ_0 is the angle between {1 0 $\bar{1}$ 1} and (1 1 $\bar{2}$ 0), and θ is the angle between any two of {1 0 $\bar{1}$ 1}. From Eq. (1), the angle between ZnO(1 0 $\bar{1}$ 1) and (0 1 $\bar{1}$ 1) is 52.188°, and the angle between ZnO(1 0 $\bar{1}$ 1) and (1 0 $\bar{1}$ $\bar{1}$) is 56.7895°. Since the angle between {1 0 $\bar{1}$ 1} and (1 1 $\bar{2}$ 0) is 40.37°, the φ angle in Fig. 2(b) can be solved.

$$\cos\theta = \frac{h_1h_2 + k_1k_2 + (1/2)(h_1k_2 + k_1h_2) + (3/4)(a/c)^2 l_1 l_2}{\sqrt{h_1^2 + k_1^2 + h_1k_1 + (3/4)(a/c)^2 l_1^2} \times \sqrt{h_2^2 + k_2^2 + h_2k_2 + (3/4)(a/c)^2 l_2^2}} \quad (1)$$

$$\varphi = 2\sin^{-1}\left[\frac{\sin(\theta/2)}{\sin\theta_0}\right]. \quad (2)$$

From the calculation, the φ angles between ZnO{1 0 $\bar{1}$ 1} peaks are alternated by 85.55° and 94.45°. As the φ-scan step in Fig. 2(a) is 1°, the distances among these four peaks are alternated by 4° and 86°. It is obvious that the alternated φ angles between adjacent peaks result from two sets of ZnO{1 0 $\bar{1}$ 1} with 90° rotation relative to each another. There is no evidence showing that in-plane orientation of ZnO(1 1 $\bar{2}$ 0) is $\pm 2°$ misaligned with LAO(1 0 0) substrate [8,9].

The appearance of two sets of ZnO {1 0 $\bar{1}$ 1} implies that there may be only two in-plane orientation relationships between ZnO(1 1 $\bar{2}$ 0) and LAO(1 0 0) substrate. Actually four possible orientation relationships can be deduced as shown in Fig. 3. Fig. 3(a) shows one of the in-plane orientation relationships of ZnO(1 1 $\bar{2}$ 0) and LAO(1 0 0), and the rest three ones are shown in Fig. 3(b). The in-plane orientation relationship can be written as ZnO[1 $\bar{1}$ 0 0]$\|$ LAO$\langle$0 1 1$\rangle$ and ZnO[0 0 0 1]$\|$LAO$\langle$0 1 1$\rangle$ if non-centro-symmetry of ZnO is not taken into consideration. Although the positive c-axis direction is not equal to negative c-axis direction, the HRXRD cannot identify the difference between them. It is why only two sets of ZnO{1 0 $\bar{1}$ 1} peaks appear in the φ-scan pattern.

Previous work has shown that ZnO(1 1 $\bar{2}$ 0) thin films can be grown on perovskite $SrTiO_3$(1 0 0) [8–10]. Since LAO has similar lattice structure and lattice constant to $SrTiO_3$, deposition of ZnO(1 1 $\bar{2}$ 0) on LAO(1 0 0) substrate is not unexpected. The rectangular ZnO(1 1 $\bar{2}$ 0) lattice can be treated as 5.627 Å length in [1 $\bar{1}$ 0 0] and 5.205 Å width in [0 0 0 1] which can match with LAO(1 0 0) along [0 1 1] and [0 $\bar{1}$ 1] (LAO[0 1 1] = 5.361 Å) lattice as a template with lattice mismatch 4.72% and 3%, respectively.

The quality of ZnO thin films grown at 450 °C was examined by HRXRD ω-scan shown in Fig. 2(c). The full-width at half-maximum (FWHM) of (1 1 $\bar{2}$ 0) peak is 4020 arcsec. The large FWHM might be mainly due to the untreated surface of LAO substrate and the twins in the substrate. Another possibility could be the large thermal mismatch between LAO and ZnO due to the difference in thermal expansion coefficients ($\sim 8\times10^{-6}\,K^{-1}$ for LAO, and c-axis $2.92\times10^{-6}\,K^{-1}$ and a-axis $4.75\times10^{-6}\,K^{-1}$ for ZnO at 300 K) [14,16].

SEM images of ZnO thin films grown at 600 °C are shown in Fig. 4. In Fig. 4(a), the weave-like surface morphology in which grains intersects with each other was formed by ZnO(1 1 $\bar{2}$ 0) grains with 90° rotation. Though the weave-like morphology dominates on the film surface, hexagonal grains are also discovered on some local regions of the film as shown in Fig. 4(b) in high magnification. The column-like ZnO(0 0 0 2) grains are related to three-dimensional growth mechanism.

The surface morphologies of ZnO thin films grown at 450 and 600 °C are shown in AFM images in Fig. 5(a) and (b), respectively. In Fig. 5(a), the bar-like and cross grains are similar to those observed in Fig. 4(a), it results from ZnO(1 1 $\bar{2}$ 0) grains having four orientation relationships with LAO(1 0 0). The surface morphologies of ZnO(1 1 $\bar{2}$ 0) support the interpretation of HRXRD φ-scan results. As the XRD pattern in Fig. 1 only shows (1 1 $\bar{2}$ 0) reflection, it is surprised to observe a hexagon-like grain in the center of the AFM image which is probably a (0 0 0 2) oriented ZnO crystallite. It seems that the ZnO(0 0 0 2) grain was deposited on the ZnO(1 1 $\bar{2}$ 0) film. No hexagonal ZnO was found in further AFM observations on the rest regions of the films. In Fig. 5(b), many large hexagonal ZnO(0 0 0 2) grains deposited at 600 °C are revealed in consistence with SEM observation in Fig. 4(b). The hexagonal grain size in Fig. 5(b) is ranged from about 0.7 to 0.2 μm. As the smaller hexagonal ZnO grains are on top of the larger ones, it is likely that 3D growth for c-plane ZnO occurs at 600 °C.

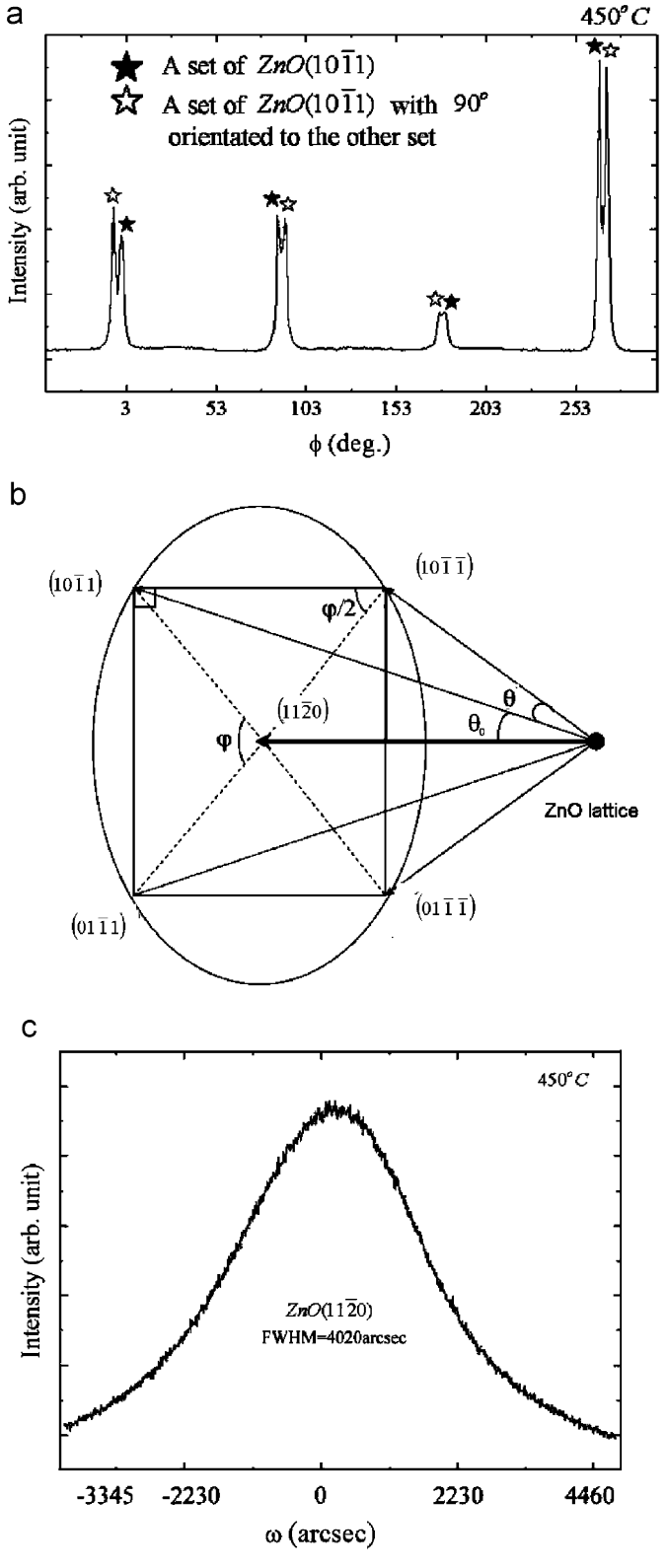

Fig. 2. High-resolution XRD data of ZnO films deposited at 450 °C (a) φ-scan showing two sets of ZnO{1 0 $\bar{1}$ 1} peaks; (b) the projection of ZnO{1 0 $\bar{1}$ 1} with ZnO(1 1 $\bar{2}$ 0) as the zone axis; and (c) ω-scan.

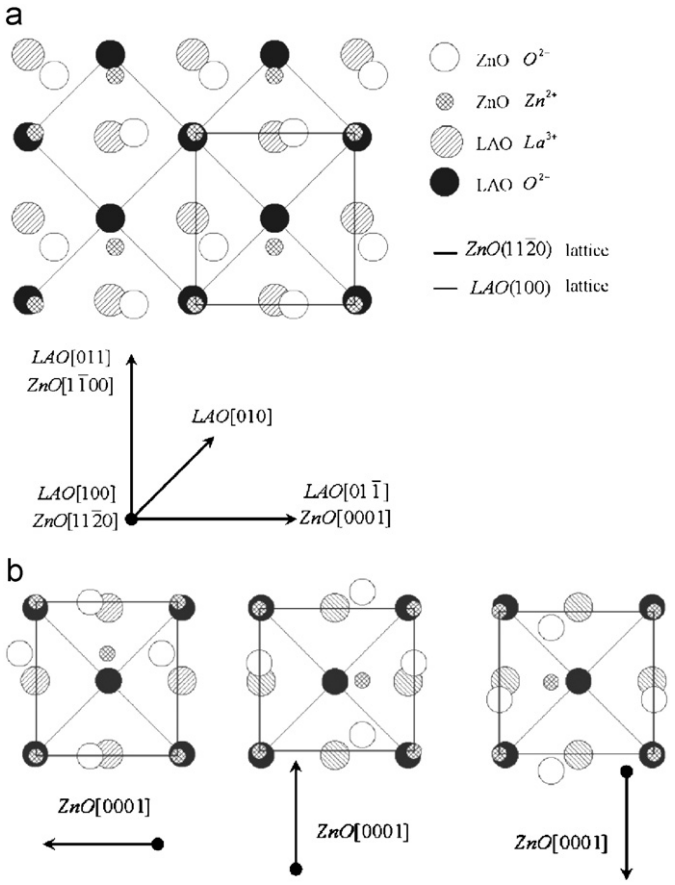

Fig. 3. Four different planar lattice relationships between *a*-plane ZnO and LAO(1 0 0). The lattice mismatch in ZnO[1 $\bar{1}$ 0 0] is 4.72%, and in ZnO[0 0 0 1] 3% with LAO.

The SEM and AFM images show the surface morphology of ZnO thin films, and the weave-like patterns confirm the 90° rotation of ZnO(1 1 $\bar{2}$ 0) in-plane growth directions. The appearance of hexagonal ZnO(0 0 0 2) grains and small column-like grains represents the different growth mechanism with ZnO(1 1 $\bar{2}$ 0) grains.

It is interesting that almost all ZnO deposited at 450 °C have *a*-plane orientation, while above 550 °C *c*-plane ZnO appears. It is likely that *c*-plane ZnO thin films preferentially grow at high temperature in MOCVD. An alternative speculation might be due to the phase transition of LAO from rhombohedral to cubic structure upon heating over 540 °C [14].

For LAO of perovskite structure, there are two possible surface terminations for {1 0 0} surfaces, La-O and Al-O_2 layers [11–14,17,18]. Yao et al. found that Al-O_2 layer terminated up to 150 °C and turned to La-O entirely at 250 °C. The mixed layer only appeared in the range from 150 to 250 °C [12]. Kawanowa et al. [19] showed that after annealing at 1300 K for 8 h for cleaning, Al-O_2 layers are dominated at room temperature, and replaced by La-O layers almost at 1000 K, but for annealing at 1300 K for 15 h, La-O layers terminated at RT and 1000 K. Both studies suggested that the surface termination change is caused by deoxidization of surface. In our case, the growth was under oxygen-rich environment but at relatively high

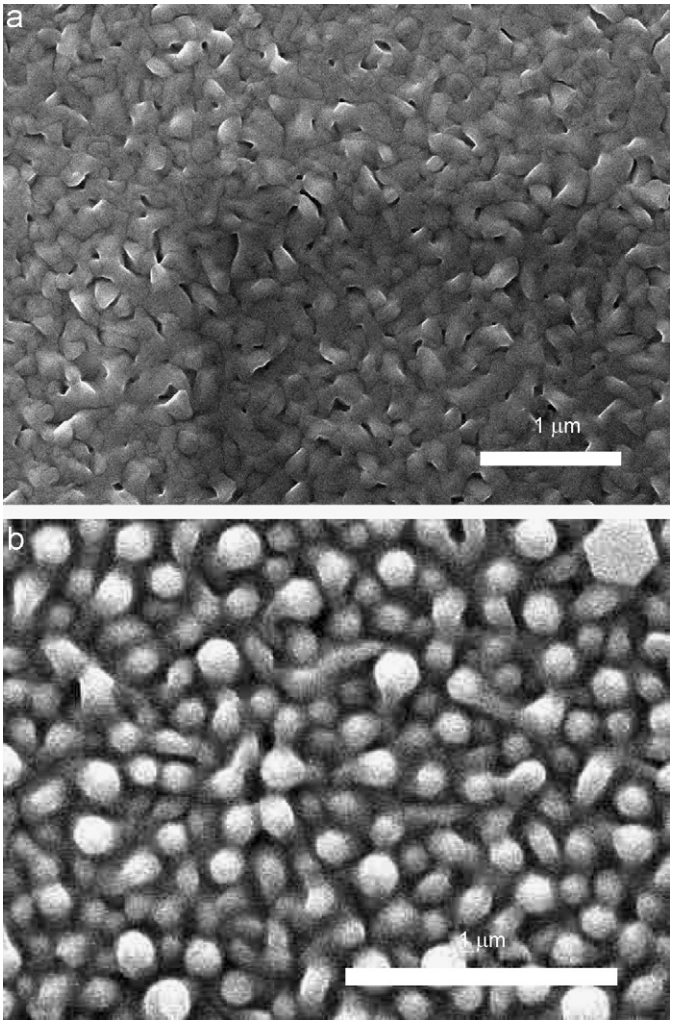

Fig. 4. SEM images of ZnO films grown at 600 °C. In (a), the weave-like surface morphology of ZnO(1 1 $\bar{2}$ 0) grains with 90° rotation. The hexagon-like small grains in (b) are ZnO(0 0 0 2)-oriented.

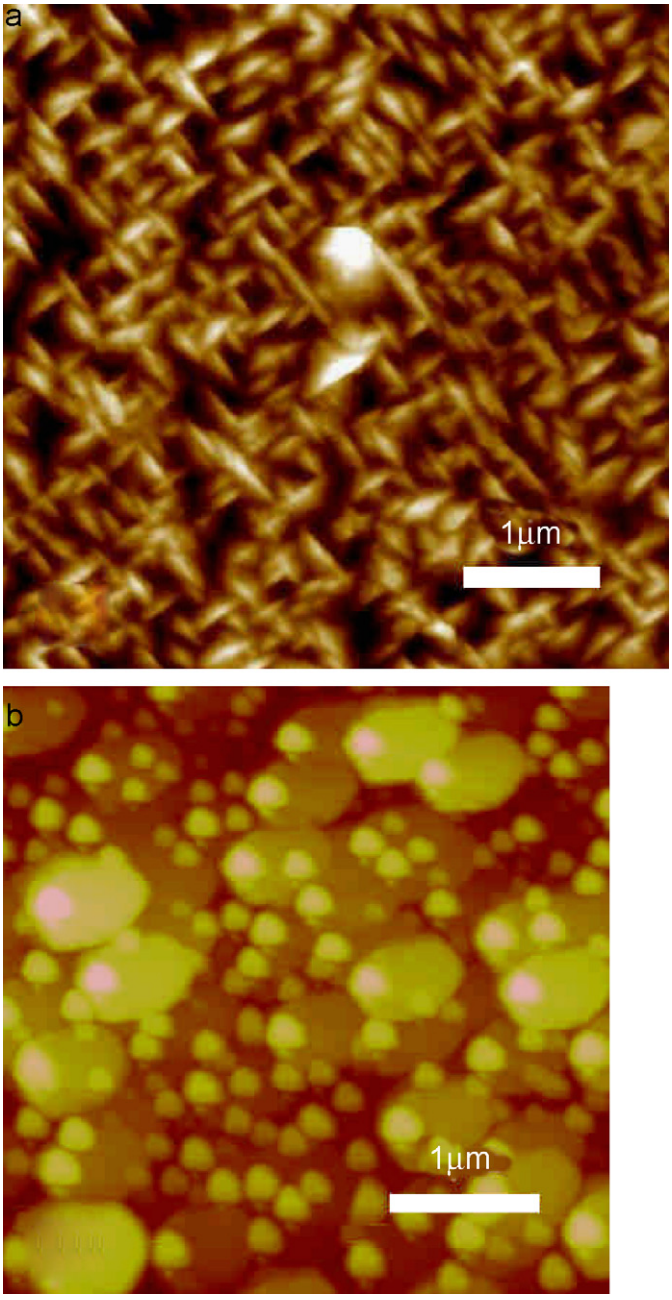

Fig. 5. (a) AFM image of (1 1 $\bar{2}$ 0) ZnO deposited at 450 °C showing the crisscross grains. (b) Hexagonal ZnO(0 0 0 2) grains grown at 600 °C.

temperature. Therefore, the transition of surface termination from Al-O_2 layer to La-O layer may occur. As a result, the LAO surface with La-O termination can then act as the template for *a*-plane ZnO deposition as shown in Fig. 3.

4. Conclusion

Deposition of non-polar *a*-plane ZnO films on LAO (1 0 0) substrate with in-plane orientations of ZnO[1 $\bar{1}$ 0 0]$\|$LAO$\langle$0 1 $\bar{1}$$\rangle$ and ZnO[0 0 0 1]$\|$LAO$\langle$0 1 1$\rangle$ has been demonstrated using MOCVD. Highly oriented a-plane ZnO films can be obtained at growth temperature of 450 °C, while the fraction of c-plane oriented ZnO grains is increased at higher temperature above 550 °C. The surface morphology shows two perpendicularly oriented ZnO domains for a-plane ZnO growth due to the four-fold symmetry of LAO(0 0 1).

Acknowledgment

The work was supported by National Science Council, Taiwan, ROC, under contract NSC 95-2221-E-009-128.

References

[1] P. Fons, K. Iwata, S. Niki, A. Yamada, K. Matsubara, M. Watanabe, J. Crystal Growth 209 (2000) 532.
[2] C.R. Gorla, N.W. Emanetoglu, S. Liang, W.E. Mayo, Y. Lu, J. Appl. Phys. 85 (1999) 2595.

[3] X.L. Du, M. Murakami, H. Iwaki, A. Yoshikawa, Phys. Status Solidi (a) 192 (2002) 183.
[4] S. Choopun, R.D. Vispute, W. Noch, A. Balsamo, R.P. Sharma, T. Venkatesan, Appl. Phys. Lett. 75 (1999) 3947.
[5] S.S. Kim, J.H. Je, J.H. Kim, Phys. Status Solidi (c) 1 (2004) 2541.
[6] T. Moriyama, S. Fujita, Jpn. J. Appl. Phys. 44 (2005) 7919.
[7] B.P. Zhang, Y. Segawa, Appl. Phys. Lett. 79 (2001) 3953.
[8] E. Bellingeri, D. Marre, I. Pallecchi, L. Pellegrino, G. Canu, A.S. Siri, Thin Solid Films 486 (2005) 186.
[9] X.H. Wei, Y.R. Li, J. Zhu, W. Huang, Y. Zhang, W.B. Luo, H. Ji, Appl. Phys. Lett. 90 (2007) 151918.
[10] M. Karger, M. Schilling, Phys. Rev. B 71 (2005) 075304.
[11] G.W. Berstresser, A.J. Valentino, C.D. Brandle, J. Crystal Growth 109 (1991) 467.
[12] J. Yao, P.B. Merill, S.S. Perry, D. Marton, J.W. Rabalais, J. Chem. Phys. 108 (1998) 1645.
[13] S. Geller, P.M. Raccah, Phys. Rev. B 2 (1970) 1167.
[14] S.A. Hayward, F.D. Morrison, S.A.T. Redfern, E.K.H. Salje, J.F. Scott, K.S. Knight, S. Tarantino, A.M. Glazer, V. Shuvaeva, P. Daniel, M. Zhang, M.A. Carpenter, Phys. Rev. B 72 (2005) 054110.
[15] R.J. Harrison, S.A.T. Redfem, A. Buckley, E.K.H. Salje, J. Appl. Phys. 95 (2004) 1706.
[16] H. Ibach, Phys. Status Solidi 33 (1969) 257.
[17] Z.L. Wang, A.J. Shapiro, Surf. Sci. 328 (1995) 159.
[18] C.H. Lanier, J.M. Rondinelli, B. Deng, R. Kilaas, K.R. Poeppelmeier, L.D. Marks, Phys. Rev. Lett. 98 (2007) 086102.
[19] H. Kawanowa, H. Ozawa, M. Ohtsuki, Y. Gotoh, R. Souda, Surf. Sci. 506 (2002) 87.